Development of HCCI natural gas engines

Kazunobu Kobayashi [a,*], Takahiro Sako [a], Yoshimi Sakaguchi [a], Satoshi Morimoto [b], Sumihiro Kanematsu [c], Kiyoshi Suzuki [d], Tohru Nakazono [e], Hiroyuki Ohtsubo [e]

[a] Osaka Gas Co., Ltd, 6-19-9, Torishima Konohana-Ku, Osaka 554-0051, Japan
[b] Tokyo Gas Co., Ltd, Tokyo 105-8527, Japan
[c] Toho Gas Co., Ltd, Aichi 476-8501, Japan
[d] Saibu Gas Co., Ltd, Fukuoka 819-0162, Japan
[e] Yanmar Co., Ltd, Shiga 521-8511, Japan

ARTICLE INFO

ABSTRACT

The possibility of turbocharging into a natural gas homogeneous charge compression ignition (HCCI) engine is experimentally investigated. Experiments are performed using a naturally aspirated engine fitted with an external supercharger and a butterfly valve for back pressure control to simulate a turbocharger. The results indicate that the thermal efficiency can be improved by raising the engine compression ratio and lowering the boost pressure. At an engine compression ratio of 21 and turbocharging pressure of 0.19 MPa, the brake thermal efficiency reaches 43%, with NOx emissions of only 10 ppm or less. Finally, the performance of the engine fitted with a newly developed turbocharger is demonstrated. As a result, 43.3% brake thermal efficiency, 0.98 MPa brake mean effective pressure, and 13.8 ppm NOx emission have been realized. This value shows the possibility that a power generating efficiency of 40% at a power output of 50 kW could be achieved when applied to combined heat and power (CHP), even allowing for energy losses in the generator and the power inverter. For practical use, the ignition timing control, operation control, including how to start or load input and ensuring durability, remain to be investigated. To clarify these issues, we have initiated the endurance test for a newly developed 25 kW HCCI package, although the engine is not supercharged.

1. Introduction

Fig. 1 shows the current gas engine CHP lineup. The range of power output is from 1 kW for residential use to several MW for industrial use. The power generation efficiency of 40% (LHV) is the average at the receiving end by thermal power generation in Japan. Our aim is to develop a decentralized generating plant with an efficiency over 40%. The power generation efficiency of large-scale CHP is over 40%, higher than the average receiving end efficiency of thermal power generation. However, the efficiency of small-scale CHP (100 kW or less) is less than 40%. Therefore, we have developed small gas engines aiming at more than 40%. One way to improve the thermal efficiency is to increase the compression ratio. The Diesel engines can be operated at the high compression ratio. However, direct fuel injection is impossible for small gas engines in small-scale CHP due to low fuel supply pressure. On the other hand, it is difficult to operate the conventional spark ignition engines at

the high compression ratio by the engine knock. Against this background, we have focused on homogeneous charge compression ignition (HCCI) combustion as an innovative technology. In the HCCI engine, ultra-lean air-fuel mixture is highly compressed by the piston and ignited at the self-ignition temperature. Then, combustion occurs in the entire combustion chamber, and the combustion rate is very high. As a result of ultra-lean combustion under a high compression ratio, high thermal efficiency and extremely low NOx emission are achieved.

HCCI combustion systems have the potential to reduce NOx emissions from diesel engines and improve the efficiency of gasoline engines under low partial load. (Najt and Foster, 1983; Thring, 1989) As such systems are also suitable for handling a wide range of fuels, the use of alternative fuels such as natural gas (Christensen et al., 1998; Jun and Iida, 2004; Sako et al., 2004; Morimoto et al., 2001) and biogas (Yamasaki et al., 2008) in HCCI systems is currently under consideration. Studies on HCCI engines have revealed that the load range over which HCCI engines can operate is limited, regardless of the fuel, by the risk of misfire, combustion instability, and engine knock. Studies have also revealed a difficulty in ensuring stable combustion over a wide range of operation,

* Corresponding author. Tel.: +81 6 6205 2757; fax: +81 6 6462 3433.
E-mail address: kazu-kobayashi@osakagas.co.jp (K. Kobayashi).

Fig. 1. Current gas engine CHP lineup.

Table 1
Engine specifications.

Engine type	Single-cylinder	Four-cylinder
Bore × stroke	112 × 115 mm	98 × 110 mm
Displacement	1132 cm^3	3318 cm^3
Compression ratio	17:1, 19:1, 21:1	
Boost pressure	0.19−0.25 Mpa	
Intake air temperature	∼573 K	
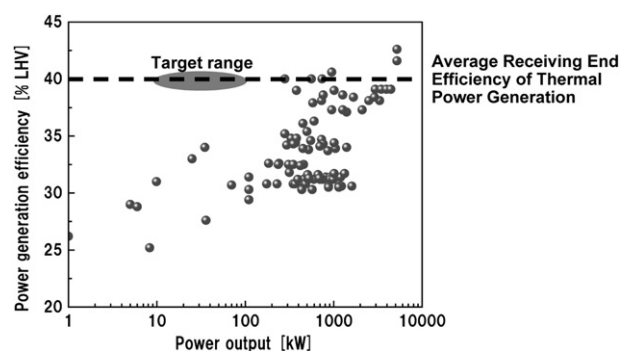
including full load. Stationary engines for combined heat and power (CHP) are required to have high thermal efficiency as well as clean emissions. On the other hand, they tend to be operated within a relatively narrow load range around rated load. Considering these circumstances, HCCI systems using natural gas may be a more fuel- and environmentally efficient option compared to conventional diesel engines in the application to CHP.

A number of attempts have been made to expand the operating range of natural gas HCCI engines, including ignition timing control by a chemical reaction-based method (Ohta et al., 2000), and the non-uniform (i.e. heterogeneous) distribution of fuel by in-cylinder direct injection (Ishiyama et al., 2002). Trials are also being conducted on combustion duration control techniques with exhaust gas recirculation (EGR) http://www.gtisoft.com. While it has been shown that both the ignition timing and combustion duration are controllable, there remains much room for improvement in terms of the mean effective pressure.

In this study, the application of a turbocharger to a small natural gas HCCI engine is examined through analysis of the performance and emission characteristics. This study reveals the strong potential of turbocharged HCCI engines.

2. Performance and combustion characteristics in supercharging

Firstly, experiments are performed with an external super-charger and a butterfly valve for back pressure control to simulate a turbocharger. With this simulated turbocharger system, the engine performance and emission characteristics were tested by varying charging factors such as the compression ratio, intake air temperature, boost pressure and equivalence ratio in order to evaluate the potential of a turbocharged HCCI engine. Finally, the performance of the engine with a new developed turbocharger was demonstrated.

2.1. Test system configuration and method

The base engine used for this test was a naturally aspirated, water-cooled, 4-cycle natural gas engine. For the supercharging trial, the engine was remodeled to allow a maximum operating in-cylinder pressure of 15 MPa. The main elements of the test system are shown in Table 1. Fig. 2 provides an outline of the test equipment. An electric heater was fitted to the intake system to maintain the intake temperature at a specified constant value, which was measured by a J thermocouple, positioned 100 mm upstream of the intake port. The intake air was pressurized to 0.8 MPa by a screw compressor, dehu-midified by a refrigeration-type air dehumidifier, and then adjusted to the specified pressure by a regulator. By the dehumidification, the reproducibility of the experiment can be improved. A butterfly valve was installed in order to apply back pressure in the exhaust system.
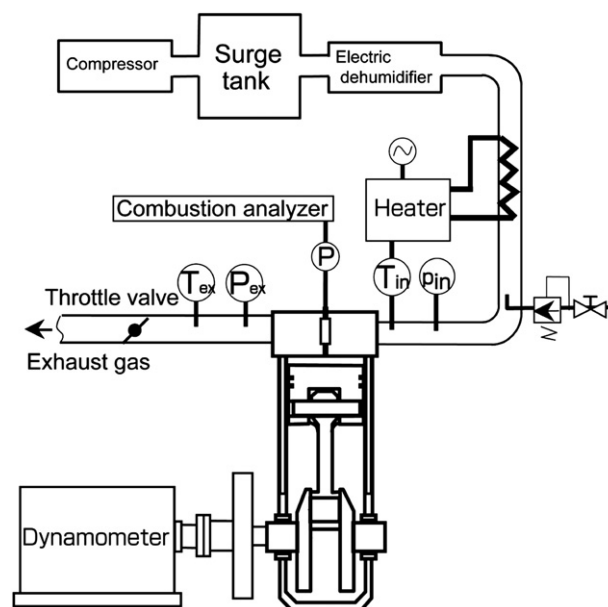

Fig. 2. Experimental setup.

The fuel used in the experiment was 13A natural gas (typical composition: CH_4 88%, C_2H_6 6%, C_3H_8 4%, C_4H_{10} 2%). After the pressure was reduced by the regulator from 0.8 MPa to 0.5 MPa, the main fuel was supplied continuously through a nozzle positioned in the intake line 1000 mm upstream of the cylinder head. To eliminate dispersion of fuel among the cylinders, a very small quantity of fuel was supplied to each of the cylinders. The nitrogen oxides (NOx) in the exhaust gas were measured by chemiluminescence analysis, carbon monoxide (CO) and carbon dioxide (CO_2) were measured by infrared analysis, and oxygen (O_2) was measured using a magnetopenumatic. The upper limit of the equivalence ratio in operation was determined by the maximum in-cylinder pressure and engine knock. The upper limit of in-cylinder pressure was determined to be 15 MPa. The knock inten-sity was defined as the amplitude of the signal wave obtained by processing the in-cylinder pressure through a band-pass filter (pass-band: 4−8 kHz), and the knock limit was defined as the equivalence ratio at which the average maximum knock intensity exceeds 0.2 MPa.

In the experiment, the opening of the butterfly valve in the exhaust system was adjusted to simulate back pressure induced by a turbocharger with efficiency of 64%. The turbocharger efficiency is defined as the ratio of compressor work to turbine work, as calculated using the specific heat of the working fluid for the measured values of intake and exhaust gas pressures, exhaust temperature, ambient temperature and air composition.

2.2. Comparison to conventional spark ignition engine

First of all, preliminary test was conducted in order to identify the potential of a turbocharged HCCI natural gas engine by using
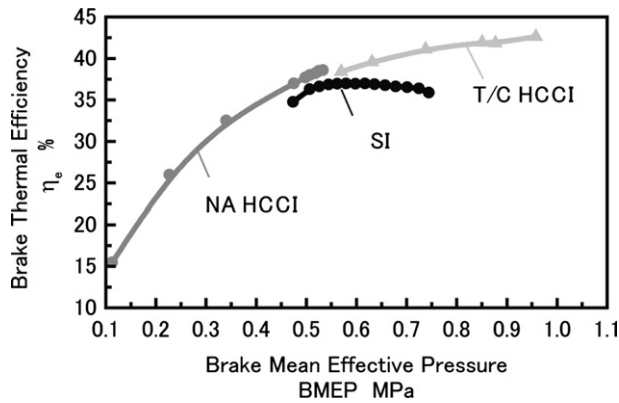
Fig. 3. Comparison between turbocharged HCCI and a conventional SI operation.

the single-cylinder test engine. Fig. 3 shows the performance of the turbocharged HCCI operation compared with that of the conventional SI operation and naturally aspired HCCI operation. Brake thermal efficiency η_e of the natural aspired HCCI operation is the same or higher than that of the conventional SI operation. However, brake mean effective pressure BMEP of natural aspired HCCI operation is decreases because of its ultra-lean operation. On the other hand, BMEP and η_e of the turbocharged HCCI operation is much higher than that of a conventional SI operation. In particular, η_e is about 6% points higher than that of a conventional SI engine. At this time, NOx is extremely low.

2.3. Performance and exhaust gas characteristics at a compression ratio of 17

In this section, the influence of parameters to mount a turbocharger with a 4-cylinder gas engine was investigated. With the compression ratio fixed at $\varepsilon = 17$, engine speed at $n_e = 1800$ rpm,
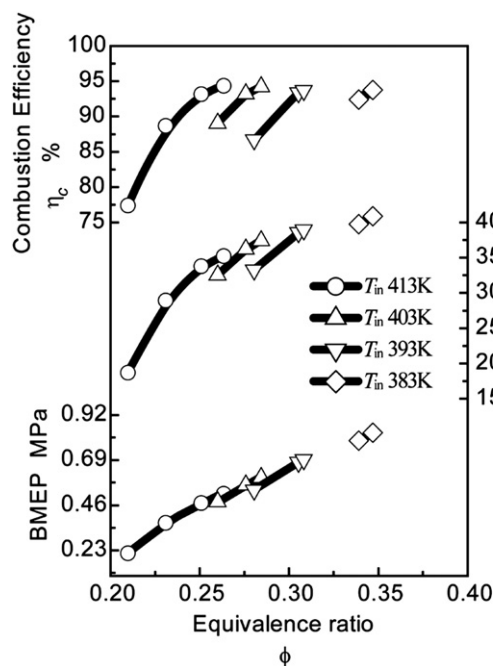

Fig. 4. Influence of intake air temperature on engine performance under supercharging conditions (engine speed 1800 rpm, compression ratio 17, and boost pressure 0.25 MPa).
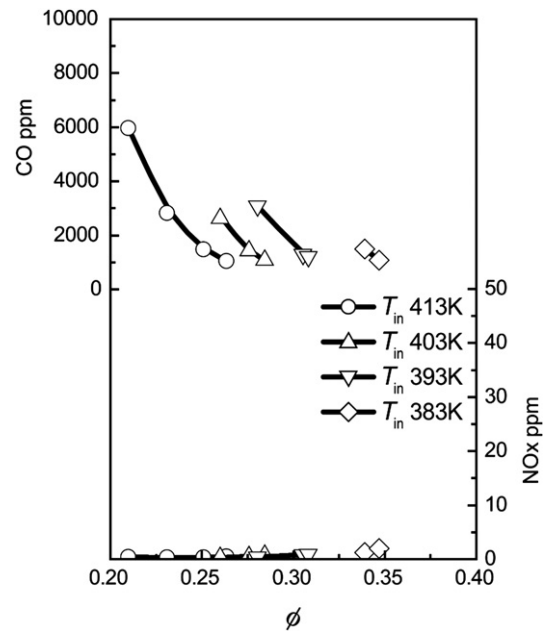

Fig. 5. Influence of intake air temperature on emission characteristics under supercharging (engine speed 1800 rpm, compression ratio 17, boost pressure 0.25 MPa).

boost pressure at $p_b = 0.25$ MPa, and assumed turbocharging efficiency at $\eta_{T/C} = 64\%$, the intake air temperature T_{in} and equivalence ratio φ were varied. Fig. 4 shows the combustion efficiency η_c, η_e and BMEP. The combustion efficiency η_c was calculated from the measured values of the exhaust gas composition. The results are shown for different values of T_{in} and φ. However, the maximum value of η_c does not depend on T_{in} and φ, as it is more or less constant at around 94%. It can also be seen that η_e improves as T_{in} becomes lower, reaching a maximum value of 40%. BMEP varies in the same way as η_c, reaching a maximum value of 0.85 MPa.

Fig. 5 shows the variation of CO and NOx in the exhaust gas with respect to T_{in} and φ. CO becomes lower as either T_{in} or φ is increased. NOx is extremely low regardless of the value of φ.

Fig. 6(a) shows the variation of in-cylinder pressure p, and heat release rate $dq/d\theta$ as the temperature T_{in} of cylinder #2 changes. The lower the value of T_{in}, the later the heat release starting point and the higher the heat release peak. The later the heat release starting point, the lower the in-cylinder pressure. The increasing lateness of the heat release starting point as T_{in} decreases can be explained as follows. The lower the temperature at the start of compression, the longer it takes to reach auto ignition temperature, which in the case of natural gas is 1000−1100 K (Jun and Iida, 2004; Sako et al., 2004) (the crank angle at auto ignition is retarded). Fig. 6(b) shows the variation of $dq/d\theta$ for each cylinder at the knock limit of $T_{in} = 383$ K. As a result of fuel charge control for limiting dispersion among cylinders, there is little deviation in the heat release starting point and peak. As shown above, η_e increases as T_{in} decreases. This is thought to be due to the reduction in cooling loss resulting from the lag in heat release starting point, an increase in the fuel charge quantity, and a change in the temperature profile due to the decrease of T_{in} (Ishiyama et al., 2002).

2.4. Performance and emission characteristics at a compression ratio of 21

A characteristic of the HCCI engine is that the brake thermal efficiency η_e improves as the intake air temperature T_{in} is reduced. At a compression ratio ε of 17, the lower operating limit for T_{in} was
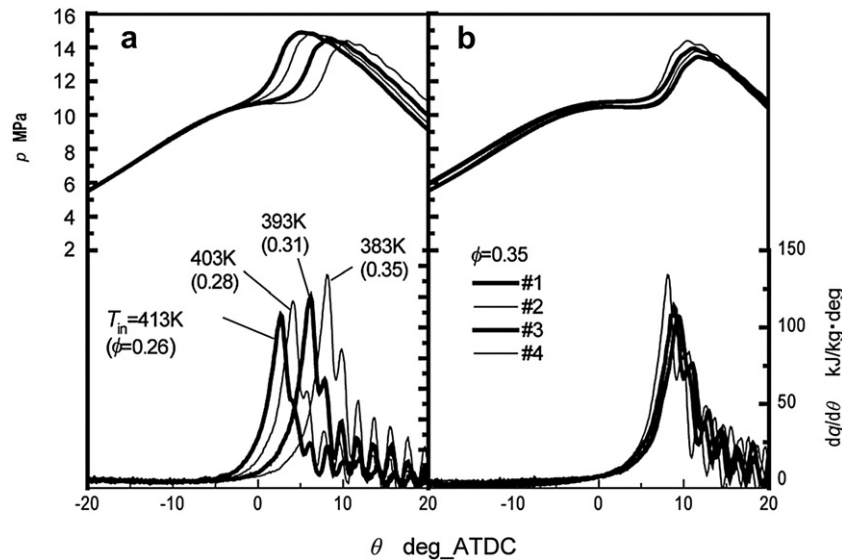
Fig. 6. In-cylinder pressure and heat release rate over time (engine speed 1800 rpm, compression ratio 17, boost pressure 0.25 MPa). (a) Change in p and $dq/d\theta$ with intake air temperature, and (b) change in p and $dq/d\theta$ for each cylinder at knock limits.

relatively high (383 K). In view of this, the authors attempted to improve η_e by extending the lower operating limit of T_{in} while increasing the compression ratio.

With the system parameters fixed at $\varepsilon = 21$, $n_e = 1800$ rpm, $T_{in} = 383$ K and $\eta_{T/C} = 64\%$, the boost pressure p_b and φ were varied. Fig. 7 shows the variation in η_c, η_e and BMEP under these conditions. It can be seen that η_c rises as p_b is reduced, and that η_e and BMEP both improve with decreasing p_b, with the former reaching a maximum value of 42%.

Fig. 8 shows the emissions from this engine. It can be seen that as the intake air temperature decreases, the operating equivalence ratio increases, which in turn results in reduced levels of CO. The NOx emission concentration is also extremely low under all conditions. The maximum value of η_c improves with decreasing p_b, due to the avoid of fuel charge reduction required at high boost

pressure to limit in-cylinder pressure. This condition also reduces the maximum attainable temperature (Jun and Iida, 2004).

In the previous tests of performance and emission characteristics, T_{in} was fixed at 353 K. Fig. 9 shows the upper limit of BMEP for all the test values of T_{in} and p_b. The fine lines in the figure represent η_e, the light gray region shows dependence of the upper operating limit on peak firing in-cylinder pressure, and the dark gray region shows the dependence of the upper operating limit on knock. From this figure, it appears to be possible to operate the engine over a relatively wide range of BMEP by suitably adjusting T_{in} and p_b. When p_b is over 0.21 MPa, the upper operating limit is determined by peak firing in-cylinder pressure, regardless of T_{in}. Below $p_b = 0.19$ MPa and $T_{in} = 373$ K, the upper operating limit is determined by engine knock. The figure also shows that in the range of BMEP from 0.75 MPa to 0.9 MPa, it is possible to attain a brake thermal efficiency higher than 42%.
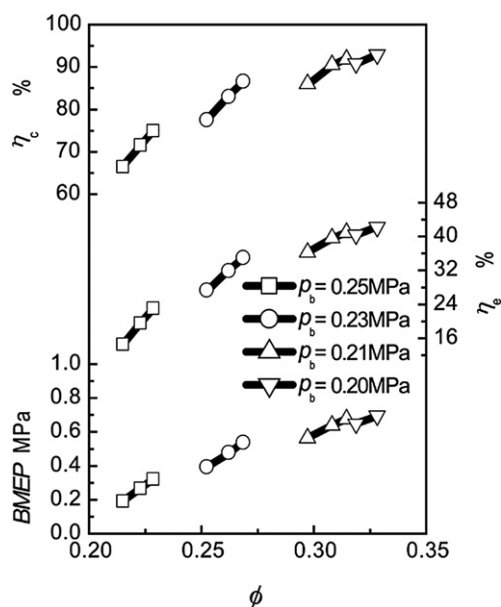
Fig. 7. Effect of boost pressure on engine performance (engine speed 1800 rpm, compression ratio 21, intake air temperature 353 K).
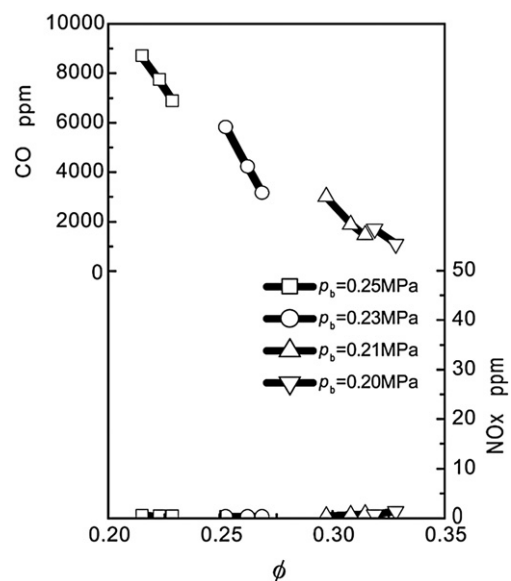
Fig. 8. Effect of boost pressure on emission characteristics (engine speed 1800 rpm, compression ratio 21, intake air temperature 353 K).
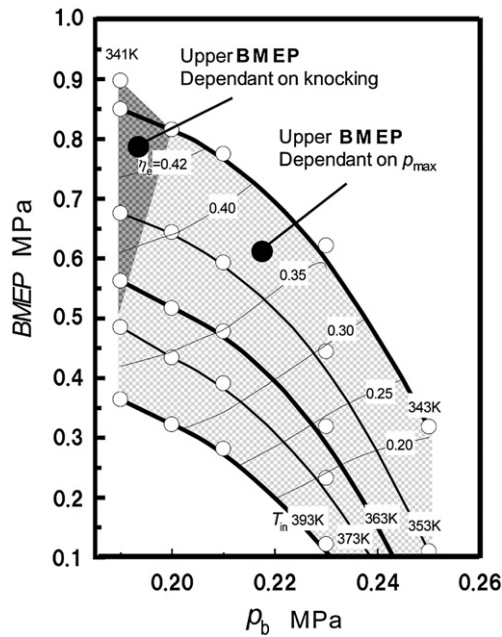
Fig. 9. Brake thermal efficiency and brake mean effective pressure with variation of boost pressure and intake air temperature at a compression ratio of 21.

2.5. Potential of natural gas turbocharged HCCI engines

Fig. 10 shows the upper operating limit values of BMEP and η_e with variation in T_{in} and φ at fixed values of ε and p_b. At $\varepsilon = 17$ and $p_b = 0.25$ MPa, the maximum value of ηe is approximately 40%. However, when ε is increased to 19 and $p_b = 0.25$ MPa, η_e decreases from the value at $\varepsilon = 17$. This is because the upper operating limit is limited by peak firing in-cylinder pressure. By setting p_b to 0.22 MPa and changing the in-cylinder pressure profile to reduce peak firing in-cylinder pressure, η_e can be improved to 41%. At $\varepsilon = 21$ and $p_b = 0.19$ MPa, the thermal efficiency can be improved even further (approximately 43%). Regardless of the values of ε and p_b, the value of BMEP at the upper operating limit is around 0.8−0.9 MPa.
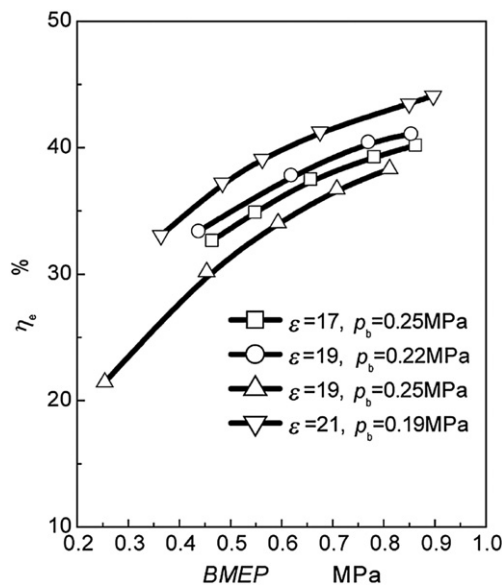
Under high thermal efficiency operating conditions, the heat release process is extremely sensitive to the fuel charge. Even a tiny change in the fuel charge can lead to knock or accidental fire, requiring a sophisticated control method to ensure continuous stable engine operation. The concentration of NOx in exhaust gas is below 10 ppm under all operating conditions. From these results it can be concluded that when the maximum in-cylinder pressure is limited, increasing the engine compression ratio to minimize the lower operating limit temperature and reducing the boost pressure makes it possible to achieve high thermal efficiency and extremely low NOx emission concentration.

2.6. Demonstration using a newly developed turbocharger

There has been no small gas engine with a turbocharger. In this study, a specialized turbocharger was newly developed. Compared with a conventional turbocharger, the size of the turbine scroll and diffuser was increased. Fig. 11 shows the test engine on which the newly developed turbocharger is mounted.

Fig. 12 shows the performance of the HCCI engine with a newly developed turbocharger. As the result, 43.3% brake thermal
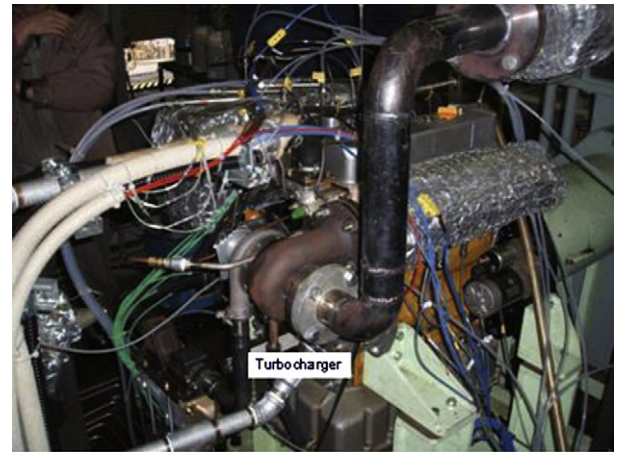

Fig. 11. Turbocharger mounted on HCCI engine.

Fig. 10. Performance of natural gas HCCI engine with simulated turbocharger (engine speed 1800 rpm, assumed turbocharging efficiency 64%).
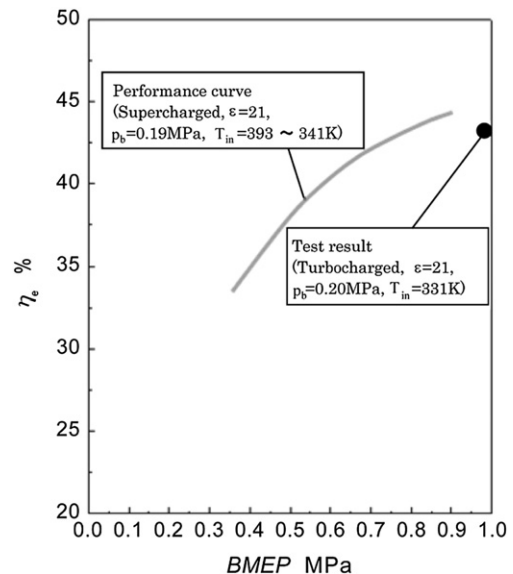

Fig. 12. Performance of natural gas turbocharged HCCI engine (engine speed 1800 rpm, compression ratio 21, boost pressure 0.20 MPa).

efficiency, 0.98 MPa brake mean effective pressure, and 13.8 ppm NOx emission have been gained. This result reveals that turbo-charging into a natural gas-fueled HCCI engine has considerable potential. Due to the characteristics of natural gas as a fuel, a high intake air temperature is necessary to achieve auto ignition, but with the application of turbocharger, intake air heating becomes unnecessary, which is another advantage.

3. Conclusions

Focused on the application to stationary engines for combined heat and power (CHP), the possibility of turbocharging into a natural gas homogeneous charge compression ignition (HCCI) engine is investigated experimentally. The results of the experiments using the simulated turbocharger indicate that when the peak firing in-cylinder pressure is limited, high thermal efficiency with extremely low NOx emission can be achieved by raising the engine compression ratio and lowering the boost pressure. The brake mean effective pressure (BMEP) of the turbocharged HCCI engine was much higher than that of the conventional SI engine.

Furthermore, the performance of the engine with a newly developed turbocharger was demonstrated. As the result, 43.3% brake thermal efficiency, 0.98 MPa brake mean effective pressure, and 13.8 ppm NOx emission have been gained. This value shows the possibility that the generating efficiency of 40% at a power output of 50 kW could be achieved when applied to CHP, even allowing for energy losses in the generator and the power inverter. These results reached our target range, and the HCCI engine demonstrated a high potential to improve dramatically the power generating efficiency of small-scale CHP (100 kW or less). Its NOx emission factor was 0.096 g/kWh. This value was extremely low, so that it was unnecessary to install exhaust treatment equipment.

The HCCI engine has a very high potential for CHP power sources. However, for practical use, the ignition timing control, operation control, including how to start or load input and ensuring durability, remain to be investigated. To clarify these issues, we have initiated the endurance test for a newly developed 25 kW HCCI package, although the engine is not supercharged. The engine has been evaluated as to the durability, including the engine control unit. Future, we intend to refine the product specifications; power output, power generating efficiency, cost, and so on.

References

Christensen, Magnus, Johansson, Bengt, Amnjus, Per, Mauss, Fabian, 1998. Super-charged homogeous charge compression ignition. SAE 980787.

Ishiyama, T., Shioji, M., Tanaka, H., Nakagawa, H., Nakai, S., 2002. Performance and exhaust emissions of a premixed charge compression ignition engine fueled with natural gas employing direct injection. JSAE Lecture Proceedings 236, 15–20 (in Japanese).

Jun, Deasu, Iida, Norimasa, 2004. A study of high combustion efficiency and low Co emission in a natural gas HCCI engine. SAE Paper 2004-01-1974.

Morimoto, S., Kawabata, Y., Sakurai, T., Amano, T., 2001. Operating characteristics of a natural gas-fired homogeneous charge compression ignition engine (performance improvement using EGR). SAE Paper 2001-01-1034.

Najt, P.M., Foster, D.E., 1983. Compression-ignited charge combustion. SAE Paper 830264.

Ohta, Y., Furutani, M., Kono, M., Kojima, M., 2000. Premixed-compression-ignition natural-gas engine. JSAE Transactions 31–32, 39–43 (in Japanese).

Sako, T., Nakai, S., Moriya, K., Iida, N., 2004. Performance and exhaust emission in a natural-gas fueled homogeneous charge compression ignition engine. Transactions of Japan Society of Mechanical Engineers, 197–203. 70-694, B (in Japanese).

Thring, R.H., 1989. Homogeneous-charge compression ignition (HCCI) engine. SAE Paper 892068.

Yamasaki, Y., Kanno, M., Nishizawa, Y., Nagata, Y., Kaneko, S., 2008. Ignition and combustion characteristics of biomass gas in a HCCI engine. Transactions of Japan Society of Mechanical Engineers, 482–484. 75–751, B (in Japanese).